

Rigorous Application of Linear Damage Concepts in Development of Improved Flexible Pavement Performance Models

STEPHEN B. SEEDS AND LUIS M. MEDUS

This paper describes the development of improved flexible pavement performance prediction models in which Miner's linear damage hypothesis was rigorously applied in evaluating original data from the AASHO Road Test. Effects of seasonal variation of soil and pavement properties were considered along with the actual steering and trailing axle loads within the linear damage framework of Miner's hypothesis. Separate models to predict the number of single- and tandem-axle loads sustained were developed using five mechanistic response criteria: asphalt concrete (AC) tensile strain, AC tensile stress, AC shear strain, AC shear stress, and roadbed soil vertical strain. The single- and tandem-axle models based on AC tensile strain had the highest overall precision, i.e., coefficients of determination (r^2) of 0.83 and 0.68, respectively. The models correlate highly with Road Test data, but they do not compare well with other performance models or even the basic AASHO Road Test performance equation. The implication is that the improved models require their own set of standard 18-kip equivalency factors for use in projecting the number of load applications that would be used in designing a flexible pavement structure.

A study for the Arizona Department of Transportation (DOT) was recently completed to evaluate increased pavement loading. In it, new procedures were developed for accurately considering the effects of load magnitude, load configuration, and tire pressure on pavement design and performance. One major task in that study was the development of improved mechanistic-empirical models to simulate the performance of flexible pavement sections at the AASHO Road Test. The models, which are based on a rigorous application of elastic-layer theory and Miner's linear damage hypothesis, were used to develop an improved set of load equivalence factors and a new mechanistic pavement design (McPAD) procedure. The focus of this paper, however, is on model development.

BACKGROUND

A damage-based pavement performance prediction model (or damage model as it will sometimes be referred to) is an equation that can be used to predict the number of load applications that can be sustained by a given pavement structure in a given environment before it reaches a certain failure criterion. (In this context, a damage model does not have to be one that is based on fatigue cracking; it only has to be one that considers cumulative load applications.) The primary and

most obvious application of a damage model is in the pavement structural design process where it provides a means for the determination of pavement layer thicknesses. Depending on the nature of the model, it also provides a basis for determining the relative effects of different wheel loads, tire pressures, and load configurations on a pavement's load-carrying capacity. The latter provision translates further into a means for converting mixed-axle-load traffic into an equivalent *design* number of axle load repetitions of a uniform magnitude.

Existing damage models vary from empirical (relying on experience or observation alone) to mechanistic (relying on engineering mechanics). Historically, pavement performance models have been empirically derived; however, there is now a trend toward developing mechanistic-empirical models. These models are based on mechanistic response factors (i.e., stress, strain, and deformation) but are statistically calibrated to observed performance.

Existing pavement damage models have one of two general criteria for failure: one is pavement condition (i.e., extent and severity of distress); the other is pavement roughness (i.e., ride quality or serviceability). The AASHTO flexible pavement performance algorithm (1) is an example of an empirical damage model having terminal serviceability as its failure criterion. Fatigue damage equations developed under NCHRP Project 1-10B (2) are examples of mechanistic-empirical models having an allowable level of cracking as their failure criterion. In general, empirical models are adequate for predicting future performance under conditions similar to those under which observations are made; however, they are not necessarily reliable for predicting performance under conditions outside those inherent in their development. Mechanistic (or mechanistic-empirical) models are better suited for prediction outside the range of the data from which they were developed, since they rely on pavement responses generated by proven theoretical models for their extrapolation. Because of the need to consider loads and tire pressures significantly higher than those considered in the past, a mechanistic approach was selected for developing the damage-based prediction models in this study.

CRITERIA FOR DAMAGE MODEL DEVELOPMENT

In addition to the use of a mechanistic-empirical approach, the following criteria were selected for the development of damage-based pavement performance prediction models for Arizona DOT:

1. AASHO Road Test data. Although 25 years old, the data base from the original AASHO Road Test experiment is still the best organized, most extensive and accurately collected set of roadway performance data.

2. Seasonal variation of roadbed soil support. To develop a mechanistic damage model with a potentially higher degree of accuracy than that of previous research efforts, it was considered essential that the seasonal variation of roadbed soil support at the Road Test be evaluated. To accomplish this, it was necessary to translate seasonal deflections and laboratory test results into pavement material properties so that the resulting variation of critical pavement stresses and strains could be considered. Miner's linear damage hypothesis (3) was assumed to be valid, thus allowing the individual seasonal damages for each AASHO Road Test section to be accumulated and used in the analysis process.

3. Consideration of the effects of steering axles independently from load axles. Since steering axle loads ranged as high as 12,000 lb at the Road Test, it was decided that their effects should be considered separately from the trailing load axles. This was accomplished within the same linear damage framework used for considering seasonal effects.

4. Serviceability as performance criterion. Traffic repetitions corresponding to a serviceability index of 2.5 were used in developing the damage models. Traditionally, pavement damage has been associated with the development of cracking; however, there was no reason not to associate it with loss of serviceability.

5. Separate damage models for single- and tandem-axle loads. This was included in the criteria for model development in order to maximize precision and to provide a better basis for evaluating the relative difference between single- and tandem-axle loads.

ANALYTICAL PROCEDURE

Several steps were accomplished in the process of developing the damage models. These steps are discussed in a logical sequence below.

Step 1: Section Selection

All of the primary AASHO Road Test flexible pavement sections consisted of cross sections having three pavement layers: asphalt concrete surface, granular base, and granular subbase. In choosing sections for detailed analysis, only those meeting the following layer thickness constraints were included: asphalt concrete surface thickness ($D_1 \geq 2$ in.), base thickness ($D_2 \geq 6$ in.), and subbase thickness ($D_3 \geq 8$ in.). These layer thickness constraints were selected in order to confine the analysis to sections having significant load-carrying capacity. Since several of these sections did not reach a terminal serviceability of 2.5 during the two-year traffic loading period, only 33 single-axle and 27 tandem-axle sections were considered.

Step 2: Season Delineation

Primary seasonal divisions were established on the basis of a detailed examination of seasonal deflections and on the find-

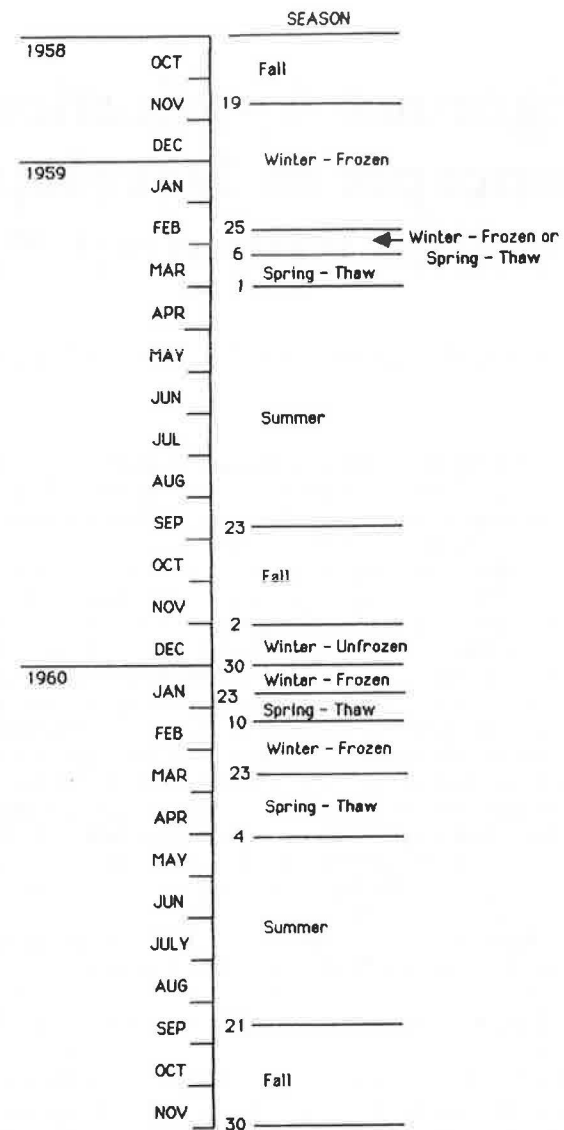


FIGURE 1 Seasonal divisions established for AASHO Road Test experiment.

ings of NCHRP Project 1-10B (2). These are depicted in Figure 1. Note that because of the different rates of thawing associated with section thickness, there is a variable division between the first hard-freeze winter and the first spring thaw. This variation was handled on a section-by-section basis. The asphalt concrete elastic modulus values for each of the seasons were based on laboratory test results and recommendations from NCHRP 1-10B (2): summer (230 ksi), fall (450 ksi), winter (1,700 ksi) and spring (710 ksi)

Step 3: Determine Cumulative Load Applications

Appendix A of AASHO Road Test Special Report 61E (4) was used to determine the cumulative number of wheel load applications sustained by each section (single and tandem) until it reached a serviceability of 2.5.

Step 4: Determine Seasonal Deflections

The graph in Figure 2 provides an example of deflection vs. time for Section 253. That plot represents the pavement surface deflection under a 30-kip single-axle load measured using a Benkelman beam. The plot indicates the critical deflection values that were selected for each season. Note that in one case (summer 1959), deflections were divided into two sub-seasons because of a significant difference in deflection at the beginning and end of the season. This subdivision was considered necessary because of the potential impact on materials characterization and was applied on several other sections.

Seasonal deflection estimates were made for all sections under the different deflection loads. Table 1 identifies the single-axle loads that were used to measure deflection on each of the sections. Recall that Lane 1 was loaded solely with single-axle load groups whereas Lane 2 was loaded primarily with tandem-axle load groups. (The tandem-axle trucks did have single-axle steering axles.)

Step 5: Characterize Seasonal Material Properties Under Deflection Loads

To characterize the seasonal material properties of each section, a computer program, MODEST-1, was developed which basically uses an elastic-layer-theory model, ELSYM5 (5), to identify a unique set of pavement layer moduli that will match the specified critical seasonal deflections and satisfy the bulk stress relationships established in NCHRP Project 1-10B (2) for base and subbase materials at the Road Test. Figure 3 provides a flow diagram of the basic iterative deflection matching process used by the MODEST-1 program. The tolerances selected for satisfying the bulk stress and deflection criteria were 5 and 3 percent, respectively.

Step 6: Solve for Seasonal Material Properties for Each Lane 1 Section

Unfortunately, because of stress (or load) sensitivity of the materials and the fact that the deflection loads were not always

TABLE 1 AXLE LOADS USED IN AASHO ROAD TEST DEFLECTION STUDIES (4)

Loop	Lane	Single Axle Load (kips)
2	1	-
	2	6
3	1	6, 12
	2	6, 12
4	1	12, 18
	2	12
5	1	12, 22.4
	2	12
6	1	12, 30
	2	12

equivalent to the actual wheel loads (compare Table 2 with Table 1), it was necessary to include this additional task as part of the materials characterization process. To predict seasonal material properties under the actual applied wheel loads, two additional computer programs were developed: STAX-1 and TANDAX-1.

Since the loads used to measure deflection matched the actual single-axle wheel loads in Lane 1, STAX-1 was designed only to estimate the material properties under the Lane 1 steering-axle loads. The diagram in Figure 4 shows roadbed soil resilient modulus vs. deviator stress, which illustrates this process for a given section during a given season. The solid line is established by plotting the modulus-deviator stress values generated in Step 5 for the two deflection loads. (The slope of the line that connects these two points is indicative of the roadbed soil's sensitivity to load.) The theoretical steering-axle relationship was generated by solving for the deviator stress values corresponding to the two previous roadbed soil modulus values. In solving for these deviator stress values, it was still necessary to satisfy the bulk stress criteria for the base and subbase materials. The intersection of the two lines defines the point at which roadbed soil stress conditions under the steering axle are consistent with the in-situ behavior of the soil. Thus, the roadbed soil resilient modulus and corresponding base and subbase modulus values at this point represent the material properties required for steering-axle load conditions.

The actual stresses and strains for each season of each segment are a by-product of the MODEST-1 and STAX-1 solutions. The results for this and the previous five steps [as they pertain to all single-axle (Lane 1) sections] are included within the draft final report to the Arizona DOT (6), but are too lengthy to include in this paper.

Step 7: Solve for Seasonal Material Properties for Each Lane 2 Section

Unlike the single-axle sections, neither the steering- nor the tandem-axle loads in Lane 2 matched the loads used to measure deflection. Consequently, it was necessary to incorporate a slightly different approach into the TANDAX-1 program to solve for the material properties required for the Lane 2 sections. As can be seen in Table 1, most of the deflections in the Lane 2 sections were measured using only a 12-kip single axle. Thus, to solve for the material properties under the steering- and tandem-axle loads, the single resilient modulus vs. deviator stress point (derived from the MODEST-1 program for the 12-kip single-axle load) had to be combined with an estimate of the roadbed soil's stress sensitivity.

The single resilient modulus vs. deviator stress point from the MODEST-1 deflection analysis is plotted, and a straight line corresponding to the estimated stress sensitivity (slope) is drawn through the point. This line represents the in-situ resilient modulus vs. deviator stress relationship for that section during that season. Since the stress sensitivity for most of the Lane 2 sections was unknown, individual estimates were based on the calculated stress sensitivity of the adjacent Lane 1 sections. For the cases where Lane 1 information was unavailable, stress sensitivity estimates were based on trends observed in other Lane 1 sections.

Once the in-situ relationship for the roadbed soil was estab-

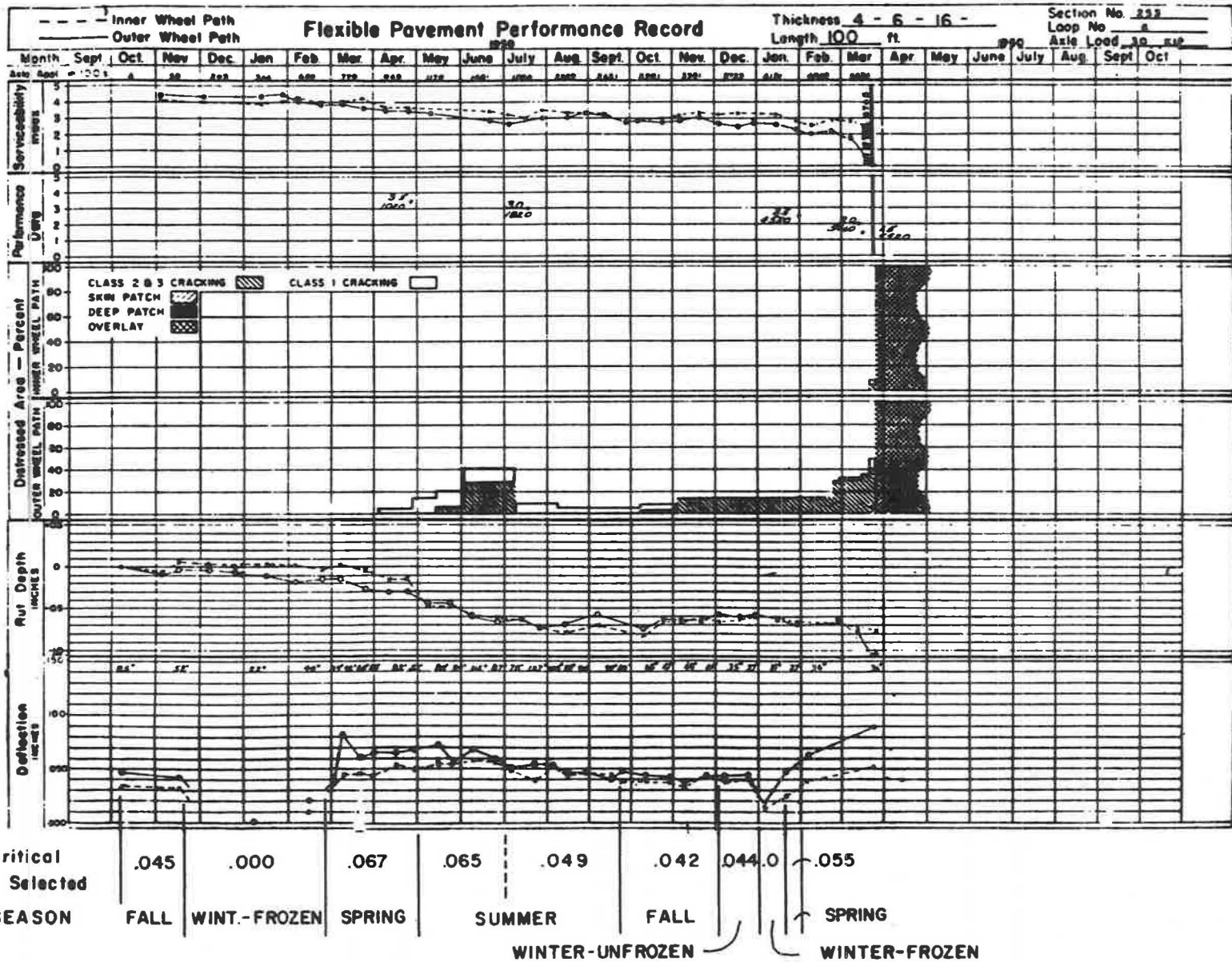


FIGURE 2 Example of average critical deflection values by season.

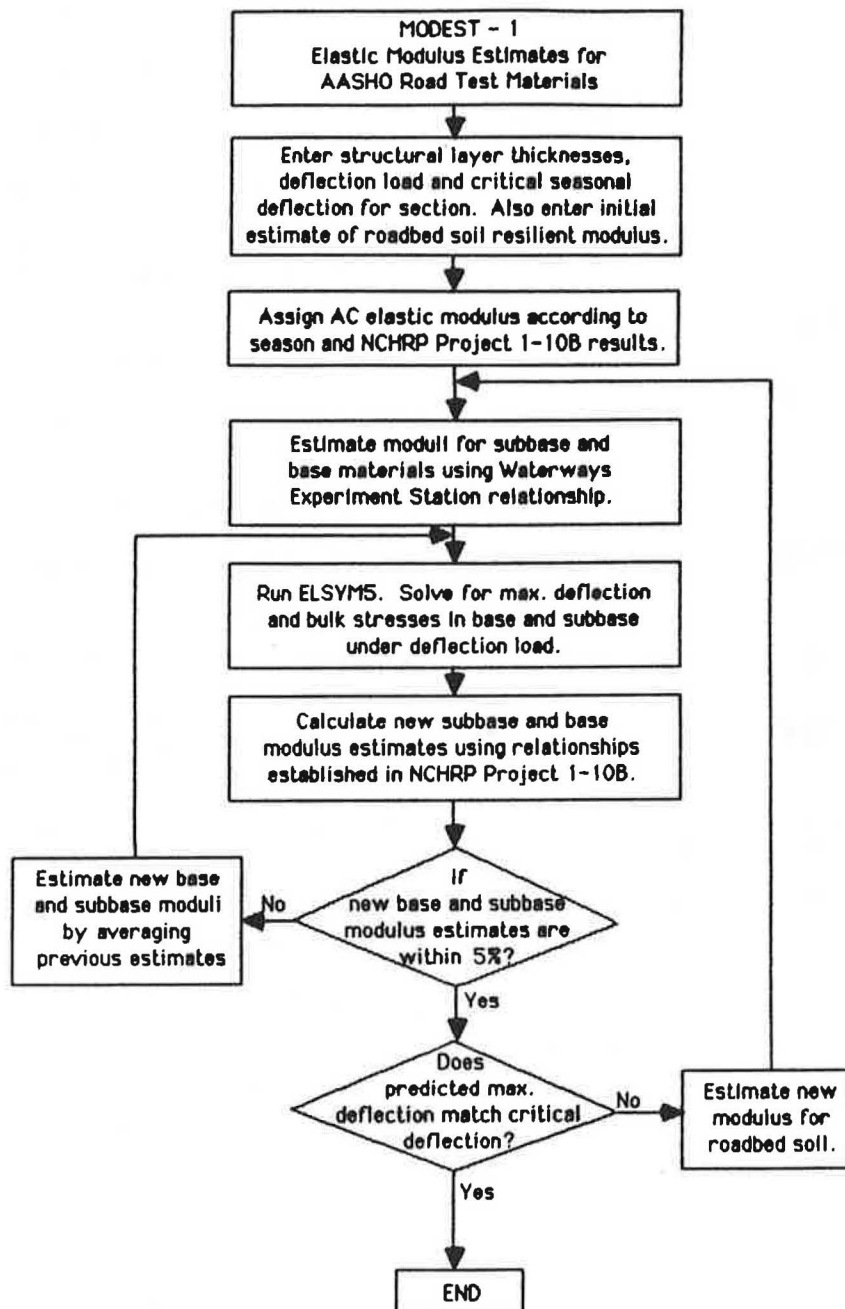


FIGURE 3 Flow diagram of MODEST-1 program.

lished, the theoretical steering- and tandem-axle relationships were generated and plotted in the same way that the steering-axle relationship was produced for the Lane 1 sections. Similarly, the intersections of the two theoretical relationships with that established for the in-situ soil represent the points at which the roadbed soil stress conditions under the given steering and tandem-axle loads are consistent with the in-situ behavior of the soil. Thus, the roadbed soil modulus values and their corresponding base and subbase moduli at these two points are the material properties required for the two particular loading conditions.











The actual stresses and strains for each season of each section are, in this step, a by-product of the TANDAX-1 solu-

tions (6). Like the single-axle results, however, they are too lengthy to include in this paper.

Step 8: Develop Single-Axle Damage Models

Separate damage models were developed for single- and tandem-axle loads. The reason for this was the desire to independently examine the effects of single and tandem axles. A combined model would have required some assumption as to the relative impact on pavement performance of positioning two single-axle loads of a given magnitude in a tandem configuration. This assumption would have introduced an addi-

TABLE 2 TEST VEHICLE LOADINGS AT AASHO ROAD TEST (4)

LOOP	LANE	WEIGHT IN KIPS			
		FRONT AXLE	LOAD AXLE	GROSS WEIGHT	
②	①		2	2	4
	②		2	6	8
③	①		4	12	28
	②		6	24	54
④	①		6	18	42
	②		9	32	73
⑤	①		6	22.4	51
	②		9	40	89
⑥	①		9	30	69
	②		12	48	108

tional source of error into the analysis and also made it impossible to use the model to examine the effects of axle configuration.

To apply a mechanistic analysis approach using elastic-layer theory and Miner's linear damage hypothesis, it was first necessary to assume a form for the damage model. Previous research efforts, including NCHRP Project 1-10B (2), suggested a form which was adopted for this study:

$$\log(N_f) = a_0 + a_1 \log(R) + a_2 \log(E_{AC}) \quad (1)$$

where, in this case,

N_f = estimated number of load repetitions to serviceability of 2.5,

R = selected mechanistic response (i.e., stress or strain),

E_{AC} = estimated elastic modulus of the asphalt concrete, and

a_0 , a_1 , and a_2 = coefficients to be determined through statistical analysis of the data.

The mechanistic responses that were considered in developing damage models (for both the single- and tandem-axle loads) include: (1) maximum asphalt concrete (AC) tensile strain, ϵ_{AC} ; (2) maximum AC tensile stress, σ_{AC} (psi); (3) maximum AC shear strain, γ_{AC} ; (4) maximum AC shear stress, τ_{AC} (psi); and (5) maximum vertical strain on roadbed

soil, λ_{RS} . The first four of these mechanistic responses were calculated at the bottom of the surface (asphalt concrete) layer and were considered in order to determine if any one in particular is a better predictor of pavement performance than the other. The last response, vertical strain at the top of the roadbed soil, was considered because of its applicability in predicting the performance of thin-surfaced pavements.

As discussed in Step 6, seasonal values for all the mechanistic responses were generated using the ELSYM5 program (5), based on elastic-layer theory. Actual values for each load and season of each section are contained within the single-axle data base presented in Appendix B of the report to ADOT (6).

The machinery for producing the a_0 , a_1 , and a_2 coefficients for the damage models was incorporated into a program called DAMOD-4. Figure 5 is a flow diagram of the major operations of this interactive program.

First, the desired mechanical response is identified and, for a specified trial a_2 value, initial values for both a_0 and a_1 are provided (operation 1). The program then goes through every season for a given section and calculates the allowable load repetitions for both the steering- and the single-axle loads (operations 2 and 3). The next two operations (4 and 5) require an explanation of a technique derived by Taute et al. (7) which uses Miner's linear damage hypothesis (3) to consider multiple seasons and nonuniform axle loads in developing a new damage model.

The linear damage hypothesis basically implies that one repetition of a given stress or strain produces the same amount of damage to a pavement whether it is applied at the beginning, middle, or end of the pavement's life. It can be expressed mathematically as follows:

$$D = \sum_{j=1}^m \frac{n_j}{(N_f)_j} \quad (2)$$

where, in this case,

D = total damage to the i^{th} section,

n_j = actual number of stress or strain repetitions of a given load during a given season,

$(N_f)_j$ = allowable number of stress or strain repetitions of a given load during a given season, and

m = product of the number of different axle loads times the number of different seasons (on the i^{th} section).

The allowable number of repetitions, $(N_f)_j$, is determined by solving the damage model (Eq. 1) for the stress or strain level corresponding to a given axle load and season. The key to estimating the a_0 , a_1 , and a_2 coefficients in the damage model, then, is to find an effective stress or strain level that would produce the same amount of damage to the section as the combination of all the axle load repetitions during the different seasons. This means that the total damage (to the i^{th} section) can also be expressed as:

$$D = \frac{\sum_{j=1}^m n_j}{(N_f)_{\text{eff}}} \quad (3)$$

where $(N_f)_{\text{eff}}$ is the allowable number of load repetitions corresponding to the "effective" stress or strain level.

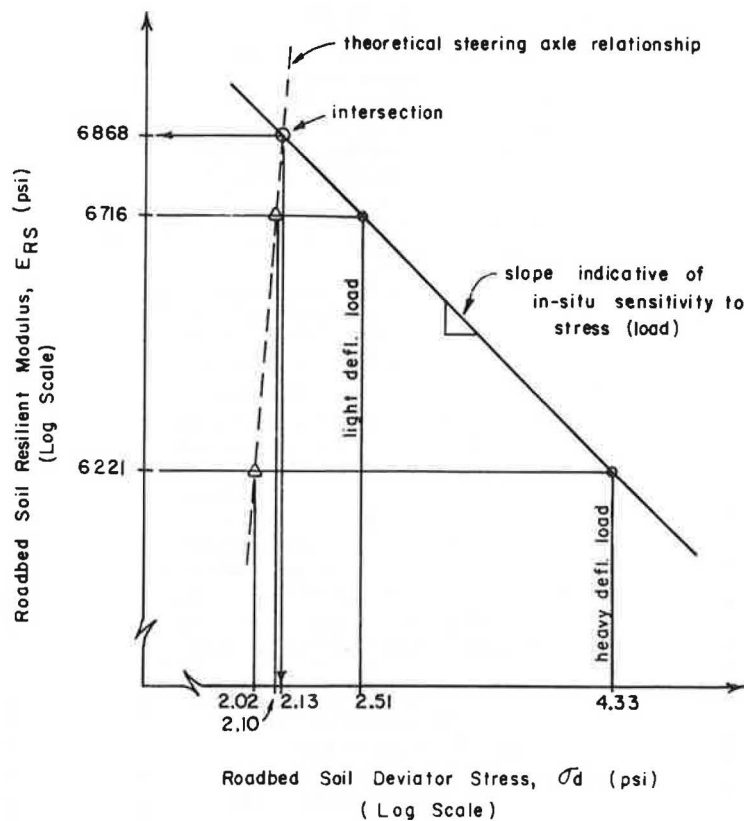


FIGURE 4 Graph of roadbed soil resilient modulus vs. deviator stress, illustrating technique used to solve for material properties under steering-axle loads in Lane 1 sections.

Rearranging the terms to solve for $(N_f)_{eff}$ and recognizing that the total damage is calculated using Equation 2 gives:

$$(N_f)_{eff} = \frac{D}{\sum_{j=1}^m n_j} \quad (4)$$

Substituting the form of the damage model for N_f in Equation 1 and solving for the effective stress or strain, R_{eff} , results in:

$$R_{eff} = \left[\frac{D}{10^{a_0} * (E_{AC})^{a_2} * \sum_{j=1}^m n_j} \right]^{1/a_1} \quad (5)$$

Note that because asphalt concrete elastic modulus, E_{AC} , is in the equation, it is necessary to calculate the effective stress or strain, R_{eff} , for a modulus value corresponding to a particular season. Since it occurs between the extreme seasons, fall (autumn) was selected as the season for R_{eff} calculations. Thus, the asphalt concrete elastic modulus value used was 450,000 psi. It should be recognized that the selection of fall as the season for R_{eff} calculations theoretically has no effect on the ultimate predictive accuracy of the damage model.

Operations 2, 3, 4, and 5 of the flow diagram in Figure 5 are performed for one Road Test section at a time. Consequently, operations 6 and 7 are included to provide a means for incrementing through each section.

Once effective stress or strain values are calculated for each section, a regression analysis (operation 8) is performed on N_f (in this case, the actual number of load repetitions experienced by the section before it "failed") vs. R_{eff} to generate new a_0 and a_1 coefficients for the damage model. A measure of the "fit" of the model to the data, known as the coefficient of determination (or r^2), is also generated as part of this regression analysis.

Operation 9 provides a test of whether the new a_0 and a_1 values are significantly different from the assumed initial values. If they are, then the process must be reexecuted using the new a_0 and a_1 values as initial estimates (operation 10). When the a_0 and a_1 values are essentially equivalent to the assumed initial values (operation 11), they represent the "best" solution for the trial a_2 value.

Table 3 is an example of output from the DAMOD-4 program for one of the initial asphalt concrete tensile strain models. For the trial a_2 value of -3.97 , eight iterations were required before the final a_0 and a_1 values matched the initial specified values. These values, then, represent the best combination of a_0 and a_1 for the selected trial value of a_2 . To get the best combination of a_0 , a_1 , and a_2 , it was necessary to try different a_2 values with the objective of finding the combination that provides the highest coefficient of determination (r^2). Table 4 illustrates how the a_2 value of -3.97 and the corresponding a_0 and a_1 values of 6.89 and -6.21 (respectively) provided the maximum r^2 . Therefore, they represent the best set of single-axle coefficients.

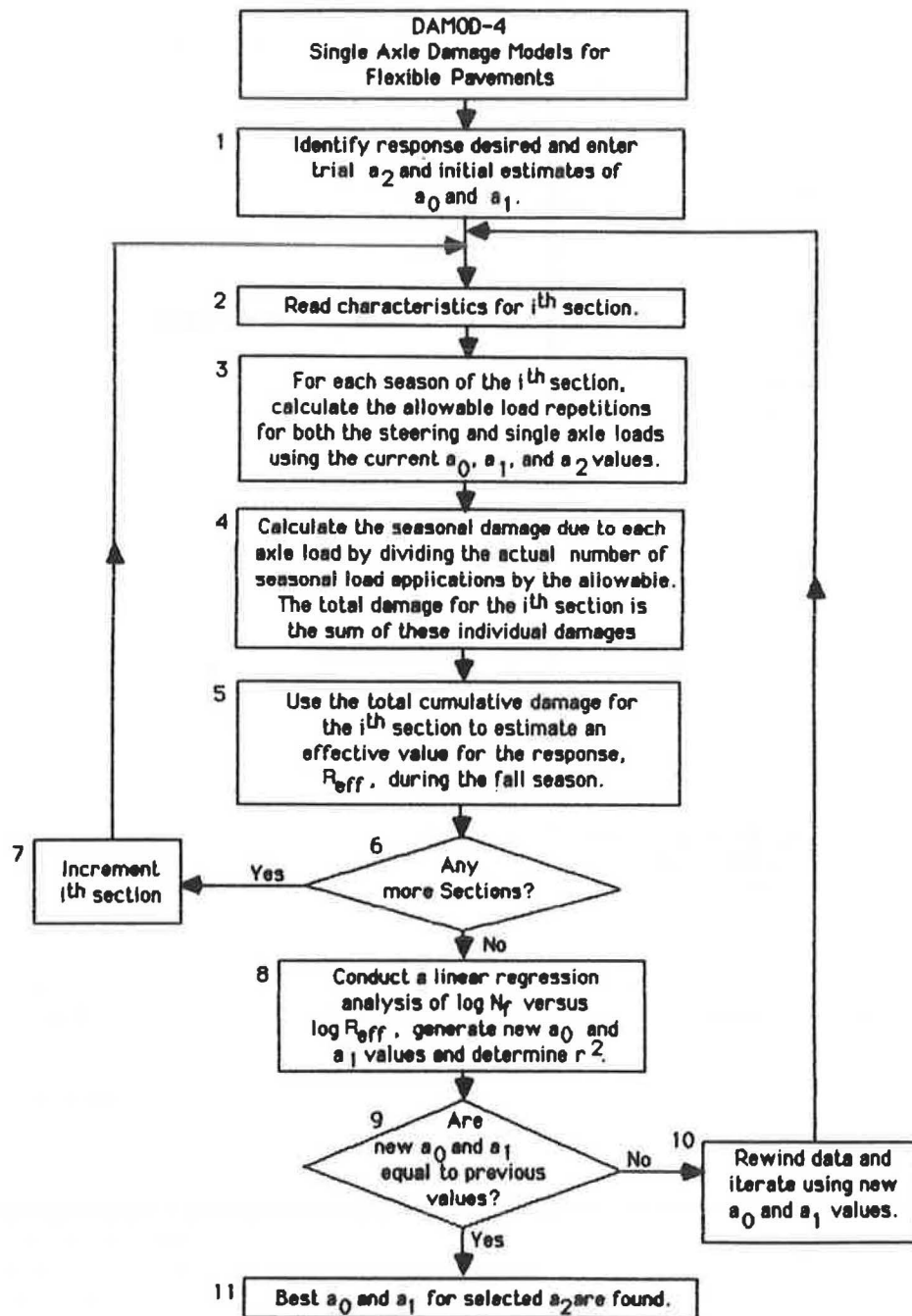


FIGURE 5 Flow diagram of DAMOD-4 program.

The DAMOD-4 analysis for single-axle loads was performed considering five different mechanistic responses (including asphalt concrete tensile strain). The results are summarized in Table 5. Figure 6 illustrates how well the tensile strain model fits the Road Test data. However, this and the other relationships were all considered *initial* or preliminary single-axle damage models. Although they are certainly valid and could be used for design or pavement performance prediction, additional equations (described next) were developed which may be more suitable.

In the process of trying to develop a single-axle damage

model based on vertical strain at the top of the roadbed soil, the analysis indicated an impractical and undue correlation with vertical strains sustained during the winter. This was probably due to the fact that the underlying materials were assigned modulus values based on engineering judgment of the properties during the winter rather than on the deflection-based materials characterization technique used for the other seasons. Whatever the explanation, it was reasoned that if pavement damage during the winter was indeed insignificant, then a suitable damage model could be developed by not considering the frozen-winter seasons in the DAMOD-4 anal-

TABLE 3 SAMPLE DAMOD-4 OUTPUT FOR PRELIMINARY SINGLE-AXLE LOAD MODEL

CRITICAL RESPONSE FOR DAMAGE MODEL: AC TENSILE STRAIN

TRIAL NO. 8

A0 6.890
A1 -6.210
A2 -3.970

SEASONAL EFFECTS:

SPRING -23.2295000
SUMMER -21.2860600
FALL -22.4432500
WINTER -24.7348800

NSEC	D1	D2	D3	TRSUM	DAMSUM	TRPRIM	STREF	X	Y	YPRIM
111	2.	6.	8.	.9315E+06	.3528E+01	264037.	.000419	-3.37760	28.41244	5.96918
155	3.	6.	8.	.9555E+06	.1587E+01	602083.	.000367	-3.43525	28.42348	5.98023
623	3.	6.	8.	.1245E+06	.4273E+00	291340.	.000413	-3.38449	27.53842	5.09517
601	3.	6.	12.	.9315E+06	.1739E+01	535789.	.000374	-3.42709	28.41244	5.96918
577	4.	6.	8.	.1140E+07	.1891E+01	602813.	.000367	-3.43534	28.50016	6.05690
625	4.	6.	12.	.1019E+07	.9352E+00	1089033.	.000334	-3.47670	28.45122	6.00796
419	3.	6.	8.	.1095E+06	.3208E+00	341288.	.000402	-3.39555	27.48267	5.03941
487	3.	6.	12.	.1155E+06	.2264E+00	510210.	.000377	-3.42367	27.50584	5.06258
471	3.	9.	8.	.1185E+06	.7254E+00	163350.	.000453	-3.34402	27.51697	5.07372
455	4.	6.	8.	.1449E+06	.9820E+00	147563.	.000460	-3.33691	27.60432	5.16107
453	4.	6.	8.	.1359E+06	.4430E+00	306764.	.000409	-3.38809	27.57647	5.13322
425	4.	6.	12.	.7575E+06	.1042E+01	726904.	.000356	-3.44843	28.32264	5.87938
417	4.	9.	8.	.2520E+06	.8012E+01	314520.	.000408	-3.38984	27.84465	5.40140
477	4.	9.	12.	.1649E+07	.1429E+01	1153994.	.000331	-3.48075	28.66034	6.21709
469	5.	6.	8.	.8400E+06	.7164E+00	1172530.	.000330	-3.48186	28.36753	5.92428
445	5.	6.	12.	.1052E+07	.6511E+00	1615064.	.000313	-3.50426	28.46506	6.02181
303	4.	6.	8.	.1200E+06	.7707E+00	155697.	.000456	-3.34067	27.52244	5.07918
323	4.	6.	12.	.1200E+06	.1071E+01	112036.	.000481	-3.31765	27.52244	5.07918
253	4.	6.	16.	.6765E+06	.1950E+01	346877.	.000401	-3.39669	28.27352	5.83027
321	4.	9.	8.	.1200E+06	.1248E+01	96156.	.000493	-3.30696	27.52244	5.07918
267	4.	9.	12.	.1620E+06	.1538E+01	105324.	.000486	-3.31333	27.65277	5.20952
309	4.	9.	16.	.1535E+07	.4167E+01	368219.	.000397	-3.40086	28.62922	6.18597
259	5.	6.	8.	.1365E+06	.6848E+00	199322.	.000439	-3.35794	27.57839	5.13513
307	5.	6.	12.	.8775E+06	.1576E+01	556653.	.000372	-3.42976	28.38650	5.94325
305	5.	6.	12.	.1890E+06	.6615E+00	285720.	.000414	-3.38312	27.71972	5.27646
327	5.	6.	16.	.1014E+07	.1700E+01	596383.	.000368	-3.43459	28.44929	6.00604
313	5.	9.	8.	.6615E+06	.1551E+01	426449.	.000388	-3.41113	28.26378	5.82053
331	5.	9.	12.	.8355E+06	.8997E+00	928599.	.000342	-3.46555	28.36520	5.92195
325	6.	6.	8.	.1530E+06	.4016E+00	380967.	.000395	-3.40324	27.62795	5.18469
257	6.	6.	12.	.1070E+07	.1150E+01	929806.	.000342	-3.46564	28.47243	6.02918
263	6.	9.	8.	.7680E+06	.8489E+00	904675.	.000344	-3.46373	28.32862	5.88536
271	6.	9.	8.	.1058E+07	.1384E+01	764358.	.000353	-3.45194	28.46754	6.02428
311	6.	9.	12.	.1005E+07	.8740E+00	1149881.	.000331	-3.48050	28.44542	6.00217

REGRESSION LINE IS:

A0 6.883
A1 -6.212
R-SQUARE .599

Notes: NSEC = AASHTO section number; D₁, D₂, D₃ = layer thickness (in.) for surface, base, and subbase; DAMSUM = total damage for section computed using a₀, a₁, and a₂; STREF = effective fall stress or strain for section; TRPRIM = allowable load applications corresponding to effective fall stress or strain; X = log₁₀ of STREF (independent variable in the regression analysis); YPRIM = log₁₀ of TRSUM (dependent variable in the regression analysis); Y = YPRIM minus the fall seasonal effect.

ysis. When this analysis was performed, the results for the vertical strain model were so remarkable that similar analyses were carried out to develop models for the other four mechanistic response variables. The results are summarized in Table 6 and a graph illustrating the relative precision for the asphalt concrete tensile strain model is presented in Figure 7.

A test of these models was made to determine if the increase

in damage that results in each section when the frozen winters are included was indeed insignificant. This test basically consisted of an examination of the differences between the damage calculated with the frozen-winter effects and those calculated without the frozen-winter effects. The results indicated that there was no significant difference for all 33 Road Test sections. Thus, it was concluded that the increase in damage

TABLE 4 SAMPLE OF OPTIMUM COMBINATIONS OF a_0 ,
 a_1 , AND a_2 FOR SINGLE-AXLE DAMAGE MODEL

Coefficients			Coefficient of Determination
a_2	a_1	a_0	(r^2)
-3.50	-6.46	3.33	0.588
-3.70	-6.35	4.85	0.597
-3.90	-6.23	6.40	0.597
-3.95	-6.21	6.78	0.597
-3.97	-6.21	6.89	0.599 (Optimum)
-4.00	-6.19	7.13	0.597
-4.10	-6.15	7.85	0.596
-4.30	-6.06	9.34	0.587

TABLE 5 INITIAL SINGLE-AXLE DAMAGE MODELS RESULTING FROM DAMOD-4
 COMPUTER ANALYSIS

Mechanistic Response Considered	Symbol (R)	Optimum Coefficients			Coefficient of Determination (r^2)
		a_0	a_1	a_2	
Asphalt Concrete Tensile Strain	ϵ_{AC}	6.89	-6.21	-3.97	0.599
Asphalt Concrete Tensile Stress	σ_{AC}	4.68	-6.40	2.80	0.615
Asphalt Concrete Shear Strain	γ_{AC}	8.96	-6.43	-4.20	0.584
Asphalt Concrete Shear Stress	τ_{AC}	6.69	-6.28	2.10	0.562
Vertical Strain on Roadbed Soil	ϵ_{RS}	(Model not possible)			

Form of Damage Model

$$\log(N_f) = a_0 + a_1 \cdot \log(R) + a_2 \cdot \log(E_{AC})$$

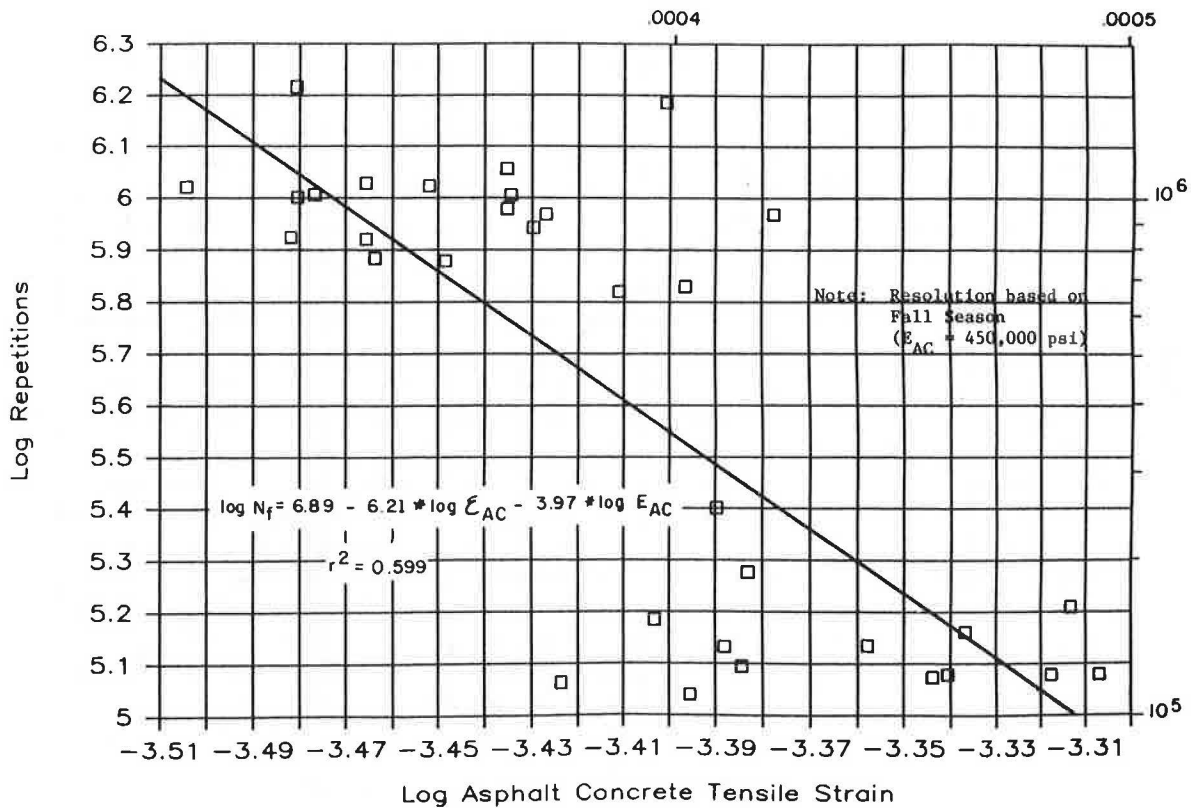


FIGURE 6 Single-axle damage model based on asphalt concrete tensile strain.

TABLE 6 SINGLE-AXLE DAMAGE MODELS RESULTING FROM DAMOD-4 COMPUTER ANALYSIS ON DATA WITHOUT FROZEN-WINTER EFFECTS

Mechanistic Response Considered	Symbol (R)	Optimum Coefficients			Coefficient of Determination (r ²)
		a ₀	a ₁	a ₂	
Asphalt Concrete Tensile Strain	ϵ_{AC}	3.25	-7.50	-4.10	0.834
Asphalt Concrete Tensile Stress	σ_{AC}	2.69	-7.47	3.60	0.841
Asphalt Concrete Shear Strain	γ_{AC}	6.61	-7.72	-4.50	0.829
Asphalt Concrete Shear Stress	τ_{AC}	3.85	-7.62	3.10	0.819
Vertical Strain on Roadbed Soil	ϵ_{RS}	-7.75	-4.28	-	0.723

Form of Damage Model

$$\log(N_f) = a_0 + a_1 * \log(R) + a_2 * \log(E_{AC})$$

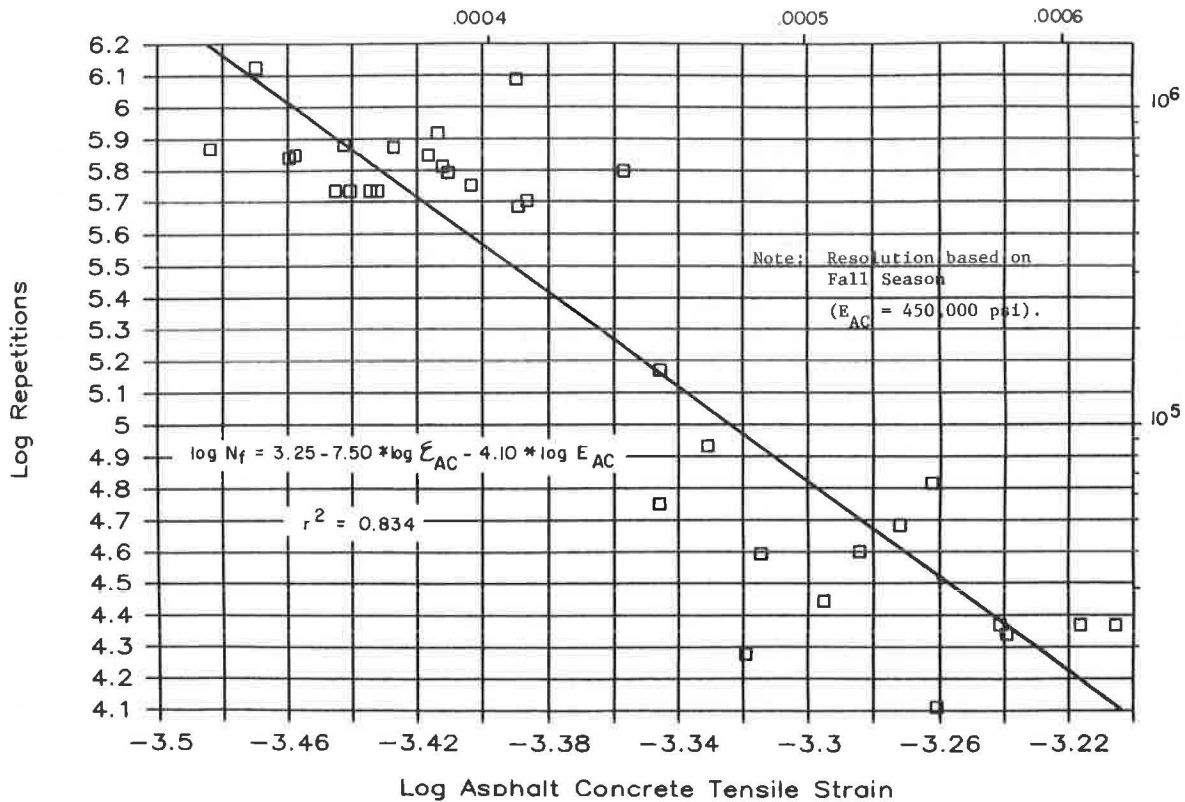


FIGURE 7 Single-axle damage model based on asphalt concrete tensile strain (frozen-winter effects not included).

due to load applications during the frozen-winter season is indeed negligible.

Step 9: Develop Tandem-Axle Damage Models

The approach to developing the tandem-axle damage models was almost identical to that for the single-axle models in Step 8. The form of the model was the same, the same five mechanistic response variables were considered, and, for consistency, load applications during the frozen-winter season were not considered. The principal difference in the analysis was in the recognition that damage due to the steering axles had to be assessed using the appropriate single-axle damage model. The necessary changes were incorporated into the DAMOD-4 program to produce DAMOD-5. The differences are in operations 1, 3, 4, and 5 (see Figure 5).

In operation 1, fixed a_0 , a_1 , and a_2 values from the single-axle model are entered along with the trial a_2 value and initial estimates of a_0 and a_1 for the tandem-axle model. In operation 3, the allowable load repetitions for the steering and tandem-axle loads are calculated using the appropriate a_0 , a_1 , and a_2 values. In operation 4, total damage is calculated with particular attention to the load configuration (steering or tandem). In operation 5, the effective stress or strain is calculated with a formula derived using the same basic approach as that used to derive Equation 5 for single-axle loads.

The final results of this step for all five mechanistic response variables are presented in Table 7.

RECOMMENDED MODELS

Based on the results of the analyses, it was recommended that the single- and tandem-axle damage models that are based on asphalt concrete tensile strain without frozen-winter effects be used both for asphalt concrete pavement design and for examining the relative effects of different loads, load configurations, and tire pressures on pavements with asphalt concrete thicknesses greater than 2 in. The predictive accuracy of all the models based on a mechanistic response in the surface layer was very high; however, the single- and tandem-axle tensile strain models had the highest combined precision. The fact that most of the experience to date with asphalt concrete damage models has been with tensile strain was another reason for recommending these particular models.

The roadbed soil vertical strain models were only recommended for the case where surface treatments or thin asphalt-concrete-surfaced pavements are being designed or evaluated. Although these models have a somewhat lower level of precision, they still explain a high percentage of the variability observed in the AASHO Road Test data.

CONCLUSION

In order to minimize the effects of extreme seasonal variations observed at the AASHO Road Test and to provide a better basis for extrapolation to heavier loads, higher tire pressures, and more repetitions, a rigorous mechanistic approach was

TABLE 7 TANDEM-AXLE DAMAGE MODELS RESULTING FROM DAMOD-5
COMPUTER ANALYSIS ON DATA WITHOUT FROZEN-WINTER EFFECTS

Mechanistic Response Considered	Symbol (R)	Optimum Coefficients			Coefficient of Determination (r ²)
		a ₀	a ₁	a ₂	
Asphalt Concrete Tensile Strain	ϵ_{AC}	0.82	-6.18	-3.0	0.676
Asphalt Concrete Tensile Stress	σ_{AC}	0.91	-5.51	3.0	0.654
Asphalt Concrete Shear Strain	γ_{AC}	5.19	-5.30	-3.0	0.580
Asphalt Concrete Shear Stress	τ_{AC}	4.75	-5.05	1.9	0.578
Vertical Strain on Roadbed Soil	ϵ_{RS}	-5.27	-3.42	-	0.649

Form of Damage Model

$$\log(N_f) = a_0 + a_1 \cdot \log(R) + a_2 \cdot \log(E_{AC})$$

used to develop improved flexible pavement performance prediction models. This has resulted in a methodology that should be better suited for use over loads, tire pressures, and environments that are well outside those of the Road Test.

As part of the Arizona DOT study, revised load equivalency factors and a computerized flexible pavement design procedure (McPAD) were developed based on the new damage models. Although the damage model coefficients (i.e., the a_1 values) are higher than those generated in past research studies, comparisons with designs derived from the Road Test performance equations indicate an excellent correspondence for Road Test conditions. The differences occur when comparisons are made for loading and environmental conditions outside the Road Test, where heavier loads, higher tire pressures, and stronger soils result in significantly different pavement structural requirements. Obviously, this means that the final results of the study will need further investigation before the models and procedures can be implemented.

ACKNOWLEDGMENTS

The authors thank the key Arizona DOT personnel, Larry Schofield, Subodh Kumar, John Eisenberg, and Rich Powers, for their support and direction on this project. They especially thank the Principal Investigator, Fred Finn, for his technical guidance and unwavering support during the rough times.

REFERENCES

1. AASHTO *Interim Guide for Design of Pavement Structures*, 1972 (Chapter III Revised, 1981), American Association of State Highway and Transportation Officials, Washington, D.C., 1981.
2. F. Finn, C. L. Saraf, R. Kulkarni, K. Nair, W. Smith, and A. Abdullah. *Development of Pavement Structural Subsystems*. Vol. I. Final Report, NCHRP Project 1-10B. TRB, National Research Council, Washington, D.C., 1977.
3. M. A. Miner. Cumulative Damage in Fatigue. *Journal of Applied Mechanics*, September 1945.
4. *Special Report 61E: The AASHTO Road Test, Report 5, Pavement Research*, HRB, National Research Council, Washington, D.C., 1962.
5. G. Ahlborn. *Elastic Layered System with Normal Loads*. Institute of Transportation Studies, University of California at Berkeley, 1972.
6. S. W. Hudson, S. B. Seeds, F. N. Finn, and R. F. Carmichael III. *Evaluation of Increased Pavement Loading*. Draft Final Report by ARE Inc. for Arizona Department of Transportation, 1986.
7. A. Taute, B. F. McCullough, and W. R. Hudson. *Improvements to Materials Characterization and Fatigue Life Prediction Methods for the Texas Rigid Pavement Overlay Design Procedure*. Research Report 249-1. Center for Transportation Research, University of Texas at Austin, 1981.